Structures and Energetics of Complexes of the *p*-Sulfonatocalix[4]arene with Ammonium, Alkylammonium, and Tetraalkylammonium Cations in Water Using Molecular Dynamics Simulations

A. Ghoufi, C. Bonal, J. P. Morel, N. Morel-Desrosiers, and P. Malfreyt*

Laboratoire de Thermodynamique des Solutions et des Polymères, UMR CNRS 6003, Université Blaise Pascal, (Clermont-Ferrand II), 24 avenue des Landais, 63177 Aubière Cedex, France

Received: November 10, 2003; In Final Form: February 23, 2004

We report results of simulations of the association process between the *p*-sulfonatocalix[4]arene and the ammonium cation. We have calculated the free energy profile of the calixarene−ammonium system in water as a function of the separation distance using the FEP formalism. The potential of mean force (PMF) profile and the MD simulations of the endpoints of this PMF curve show that the ammonium cation is not complexed by the calixarene. In addition, we have studied the complexes of the calixarene with methylammonium, tetramethylammonium and tetraethylammonium cations in water. We have shown the insertion of the tetraalkylammonium cations into the cavity of the calixarene by calculating the number of alkyl groups inside the cavity. A correlation between the number of inserted alkyl groups and the experimental enthalpy of complexation has been found. We have shown that, at the structural and energetic levels, the United Atom (UA) and All Atom (AA) descriptions give similar results for the tetramethylammonium complex. The influence of the pH on the structure and energetics of the tetramethylammonium and tetraethylammonium complexes has also been examined.

1. Introduction

Synthetic water-soluble macrocyclic receptors can be useful as mimics of biological systems but also as simple models for the identification of the factors that govern the formation of supramolecular complexes. Interactions between aromatic units and positively charged nitrogen groups being frequent and important with proteins, the *p*-sulfonatocalixarene (Figure 1), which consist of phenol units, appear as an interesting class of synthetic hosts for biorganic and biomimetic chemistry.[1] This explains why the binding of the *p*-sulfonatocalixarenes with tetraalkylammonium cations has received much attention during the last years,[2] particularly in relation with the recognition of neurotransmitter acetylcholine by acetylcholinesterase. It has indeed been suggested that this recognition could be stabilized by cation−π interactions between the positively charged quaternary ammonium group of acetylcholine and the aromatic residues of the enzyme binding site that form a narrow pocket around the guest.[3]

To understand how the *p*-sulfonatocalixarene and the R_4N^+ cations assemble and to identify the stabilizing factors, a complete thermodynamic characterization of the binding process was carried out by microcalorimetry at 25 °C. The Gibbs free energies, enthalpies and entropies of binding of the tetraalkylammonium cations by the *p*-sulfonatocalix[4]arene in water were determined at pH 2 and 7.5.[4,5] For comparison, the bindings of parent guests such as the alkylammonium cations and the alkanols were also studied.[4,6] Increasing the pH from 2 to 7.5 gave rise to slightly positive additional enthalpic and entropic contributions but did not modify the thermodynamic trends. Our results, combined with those reported in the literature[7,8] showed that for all these guests the binding process is enthalpy-driven ($\Delta_rH° \ll 0$ and $T\Delta_rS° < 0$ or > 0). This thermodynamic behavior is in sharp contrast to that observed for processes involving purely ionic binding ($\Delta_rH° > 0$ and $T\Delta_rS° \gg 0$)[4,9] or classical hydrophobic interactions ($\Delta_rH° \approx 0$ and $T\Delta_rS° > 0$),[10,11] which are markedly entropy-driven.

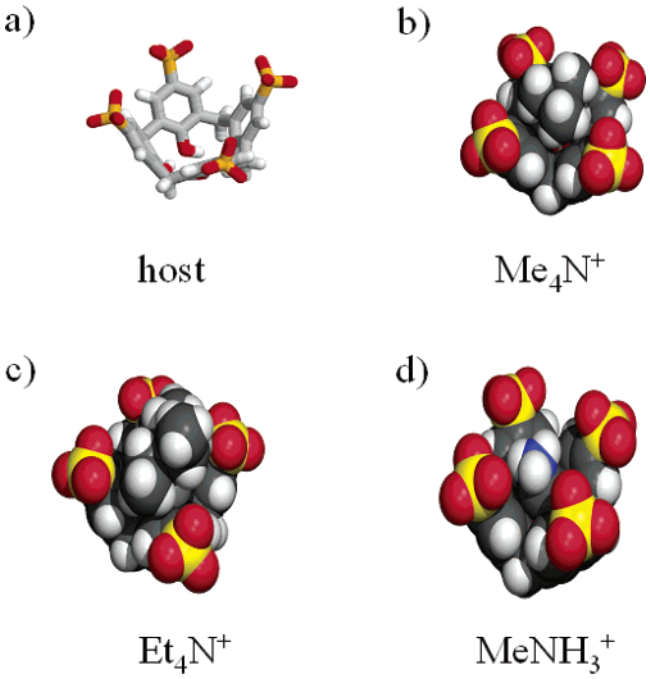

Figure 1. (a) Skeleton scheme of the *p*-sulfonatocalix[4]arene anion. Snapshots of complexes of the calixarene with (b) the Me_4N^+ cation described using the AA model, (c) the Me_4N^+ cation with the AA model, and (d) the $MeNH_3^+$ cation modeled with the UA description.

* Corresponding author. E-mail: patrice.malfreyt@univ-bpclermont.fr.

10.1021/jp037411x CCC: $27.50
Published on Web 03/26/2004

Because no heat effect was detected for NH_4^+,[4,6] we concluded that this cation is not significantly complexed by the *p*-sulfonatocalix[4]arene, although this does not constitute definite evidence because purely entropic bindings, though scarce, can exist. This is an important point that needs to be confirmed. The replacement of one of the hydrogen atoms of the ammonium ion by an alkyl group makes complexation possible. We showed[6] that, within the RNH_3^+ series (R: Me to Hept), the enthalpy of binding becomes more favorable as the length of the alkyl chain increases, reaching a plateau for $PenNH_3^+$ (at about -20 kJ mol^{-1}), which suggests that the pentyl group gives the optimal fit of the host cavity. Interestingly, we showed[6] that the enthalpy for the binding of a RNH_3^+ cation is very close to that for the binding of the corresponding neutral ROH molecule (for instance, $\Delta_r H°[C_3H_7OH] = -16.6 \pm 0.8$ kJ mol^{-1} and $\Delta_r H°[C_3H_7NH_3^+] = -16.9 \pm 0.1$ kJ mol^{-1}). This led us to conclude that it is the inclusion of the alkyl chain into the host cavity, through van der Waals interactions, that governs the binding process. The fact that the affinity is much higher for the RNH_3^+ cation than for the neutral ROH essentially results from the favorable entropic contribution associated with the desolvation of the NH_3^+ group of the guest and the SO_3^- groups of the host upon their ionic interaction. We showed, except for Et_4N^+, which exhibits remarkably negative enthalpy and entropy of binding, that the thermodynamic behavior of the R_4N^+ cations is, on the whole, similar to that of the RNH_3^+ cations, the governing factor being the inclusion of alkyl groups into the cavity.[4,5] This is particularly true for the largest species which bear propyl or butyl groups. However, when we compare Me_4N^+ with $MeNH_3^+$ we see that the enthalpy of binding is much more favorable and the entropy of binding slightly less favorable for Me_4N^+.

Molecular modeling should provide an explanation of the observed thermodynamic behaviors. In a recent molecular dynamics simulation of the association of the *p*-sulfonatocalix[4]arene with inorganic and organic cations, we examined the structures of the R_4N^+ complexes (R: Me to Pr) in water at pH 2.[12] To our knowledge[13] this was the first MD simulation of this type of complexes in water. We showed that Me_4N^+ is deeply inserted into the cavity of the *p*-sulfonatocalix[4]arene. As concerns Et_4N^+, we saw that one of the alkyl chains is close to the center of mass of the calixarene, two of them are located near the upper rim and the fourth one is outside the cavity. For Pr_4N^+, we showed that one chain is inside whereas the three others are outside the cavity.

The objectives of the present work are 2-fold. First, we would like to give an answer to the possible association between the *p*-sulfonatocalix[4]arene and the ammonium cation. The microcalorimetry experiments indeed suggest that the ammonium cation is not complexed by the calixarene, but this does not preclude the possibility of a purely entropic binding. This point may be clarified by molecular simulations. MD simulations differing in the initial position of the ammonium cation have thus been undertaken. To give a quantitative answer to the association and dissociation process involving the ammonium cation, the change of the free energy as a function of the separation distance between the host and guest is examined. This is done by calculating the potential of mean force (PMF) between the host and guest. Second, we want to investigate more deeply the structure of the *p*-sulfonatocalix[4]arene with tetraalkylammonium cations. ^{1}H and ^{13}C NMR studies[7] have underscored the inclusion of the cation into the calixarene cavity. Throughout the simulations of the complexes of the calixarene with alkylammonium and tetraalkylammonium cations, we intend to highlight the insertion of alkyl groups within the cavity and to relate the experimental $\Delta_r H°$ to the number of inserted atoms. We also check the influence of pH on the structure and energetics of the tetramethylammonium and tetraethylammonium complexes. Besides, we compare, at the energetic and structural levels, the descriptions of the Me_4N^+ cation using both an all-atom (AA) representation and a united atom (UA) version.

The outline of the paper is as follows. In section 2, we present succinctly the potential model with the methodology. The first part of section 3 contains the results of the MD simulations of the *p*-sulfonatocalix[4]arene with the ammonium cation and of the calculation of the potential of mean force between the host and guest. The second and the third parts of this section present the studies of the complexes with the tetramethylammonium and tetraethylammonium cations, respectively. We finish section 3 with the complex formed between the calixarene and the methylammonium cation. We conclude in section 4 with a summary of the present results and a brief description of the future work.

2. Potential Model and Computational Methodology

The *p*-sulfonatocalix[4]arene anion is, in all cases, modeled using the all-atom (AA) version of the Cornell force field AMBER.[14] The overall potential function is of the form

$$U(r^N) = \sum_{\alpha,\beta} U_b(r_\alpha, r_\beta) + \sum_{\alpha,\beta,\gamma} U_\theta(r_\alpha, r_\beta, r_\gamma) + \sum_{\alpha,\beta,\gamma,\delta} U_\phi(r_\alpha, r_\beta, r_\gamma, r_\delta) + \sum_{i=1}^{N-1} \sum_{j>i}^{N} U_{nb}(r_{i,\alpha}, r_{j,\beta}) \quad (1)$$

where U_b,U_θ, U_ϕ, and U_{nb} represent the bond, angle, torsion, and nonbonded interactions, respectively. The bond and valence angle potentials are represented by quadratic functions, whereas the torsional interactions are represented by a truncated Fourier series. The intramolecular or intermolecular interactions consist of a van der Waals repulsion−dipersion term calculated using the Lennard-Jones (6−12) potential and a charge−charge interaction. The C−H and O−H covalent bonds are kept of fixed length by use of the SHAKE algorithm[15] and the aromatic rings are kept planar using six improper torsional potentials. In the AMBER force field, the nonbonded interactions between atoms separated by exactly three bonds (1−4 van der Waals interactions) are reduced by a factor of 0.5.[14] The bond, bond angles, dihedral angles, and LJ parameters for the sulfonate groups are taken from ref 16. The Lennard-Jones potential parameters for the interactions between unlike atoms are calculated by using the Lorentz−Berthelot mixing rules. The water molecules are represented with the TIP3P model.[17]

The system consists of one *p*-sulfonatocalix[4]arene anion with a monovalent cation and 900 water molecules, leading to an average cubic box size of 31 Å. At pH 2, the charge of the macrocycle is -4 due to the four sulfonate groups located on the upper rim of the calixarene whereas it is -5 at pH 7 with the additional deprotonation of one phenolic hydroxy group on the lower rim. To ensure the electroneutrality, 3 Na^+ and 4 Na^+ are added at pH 2 and 7, respectively. The sodium ions are located in such a way that the $Na^+\cdots Na^+$ and $Na^+\cdots$calixarene distances are larger than the cutoff radius. We check that these distance criteria are satisfied during the acquisition phase. The calixarene is located at the center of a cubic box. The Me_4N^+, Et_4N^+, and $MeNH_3^+$ cations are initially placed so that the distance between the cation and the center of mass (com) of the SO_3^- groups are about 4 Å. Water molecules are then added

with random orientations. As a result, at the beginning of the equilibration phase, some water molecules are present into the cavity of the calixarene and between the host and guest. The system is relaxed by using MD simulations at zero temperature. The periodic boundary conditions are applied in all the three dimensions. The long-range electrostatic interactions[18] are calculated using the Ewald summation technique with the range of the real space interaction controlled by the convergence parameter $\alpha = 0.2651$ within a relative error of 10^{-6}. The reciprocal space summation is thus performed using $k_{max} = \{8 \times 8 \times 8\}$.

The atomic charges on the calixarene anion have been fitted to reproduce the molecular electrostatic potential created around the uncomplexed calixarene at the HF level with a 6-31G basis set on a number of potential energy surfaces, generated from 1.4, 1.6, 1.8, and 2.0 times the van der Waals atomic radii. We use as a grid-based method the CHELPG[19] procedure, which produces a symmetric grid of points when the structure of the molecule is symmetric. The quantum ab initio calculations are carried out using the GAMESS package.[20] Compared to the partial charges calculated using the AM1 Hamiltonian in our previous paper,[12] we note no significant change in the magnitude of the atomic charges between the AM1 and ab initio calculations. The only differences we observe concern the sign of the H atom charge of the aromatic ring which changes from +0.061 (AM1) to −0.114 (ab initio) in electron units. The partial charges on the NH_4^+, Me_4N^+, Et_4N^+, and $MeNH_3^+$ ammonium cations have been taken from ref 21 and have been calculated using the 6-31G* basis for the UA and AA models.

The equations of motions are integrated using the Verlet Leapfrog algorithm scheme in the NpT ensemble ($p = 1$ atm and $T = 298$ K) with a 2 fs time step. We use the Berendsen algorithm[22] with coupling constants 0.1 ps (temperature) and 0.5 ps (pressure). We use the multiple time step algorithm[23] in conjunction with the Verlet neighbor list. The interval for computing the secondary force is taken equal to 5 steps with a larger cutoff ($r_c = 12$ Å) whereas the primary force is calculated every time step within a cutoff of 8 Å. The Verlet list sphere radius is fixed to 14 Å. The simulations are performed using the DL_POLY_MD package.[24]

3. Results and Discussions

3.1. Association/Dissociation Process with NH_4^+ Cation. The results of the microcalorimetric measurements suggest that the ammonium cation is not significantly complexed by the *p*-sulfonatocalix[4]arene in water.[4,6] To check that, we perform two MD simulations different by the starting configuration over 1 ns. An initial configuration is built with the ammonium cation located inside the cavity of the calixarene by superimposing the two centers of mass. A second starting configuration is generated with the ammonium cation located at 12 Å from the center of mass of the calixarene. To describe the shape of the calixarene molecule, we need to calculate the asphericity coefficient.[12] This calculation gives an average value close to 0.08, indicating that the conformation of the calixarene can be assimilated to a sphere. The radius of the sphere is then equal to the root-mean-square radius of gyration (≃5 Å), the com of the calixarene defining then the center of the sphere. This means that the size of the cavity of the calixarene along a particular direction is about 10 Å. The analysis of the trajectory of the distance between the centers of mass of the calixarene and ammonium cation from the initial conformation in which the com coincide show that the cation is, on average, more or less located inside the cavity during 600 ps (Figure 2a). From this time, the cation starts to leave the cavity of the calixarene with a distance increasing continuously up to 20.7 Å. This leads us to decouple this MD simulation into two periods, the first period ($t < 600$ ps) characterized by the insertion of the cation into the cavity and the second one ($t > 600$ ps) for which the cation leaves the cavity. From the starting conformation for which the host and guest are 12 Å apart, we get a mean distance that oscillates around 14.7 ± 2.1 Å with a maximum value of 22.4 Å and a minimum value of 8.4 Å. The guest in this situation will be referred to as the uncomplexed cation.

In what follows, we investigate thoroughly the period of time during which the cation is inserted into the cavity. The ammonium N−water O radial distribution functions (rdfs) are calculated from MD simulations differing in the starting location of the ammonium cation and are shown in part b of Figure 2. As a comparison, we give the radial distribution function of the free cation in solution. We check that small differences appear in the first hydration shell of the cation and concern only the height of the first peak with an unchanged position. In fact, we see that the rdf calculated for the first 600 ps, which characterizes the insertion of the cation, presents a smaller peak. The integration of this peak yields a hydration number equal to 5.3 for the cation into the cavity. This number increases to 6.5 for the free cation and for the uncomplexed cation.

The number of hydrogen bonds between the cation and water molecules is estimated at 4.7 and 3.2 for the free cation and the inserted cation, respectively. This type of bond can form between the ammonium cation and water molecules if the following distance criteria are satisfied: $N-H\cdots OH_2 < 2.45$ Å and $H_4N^+\cdots OH_2 < 3.5$ Å. We also check that the nitrogen−oxygen−hydrogen angle is always less than 30° [25,26] when the two distance criteria are satisfied. These results suggest that the first hydration shell of the cation is not significantly perturbed upon insertion into the cavity. The second peak shows some marked differences with the rdf of the cation into the cavity. The integration of the second peak gives an average number of water molecules equal to 18 whereas it is equal to 25 for $t > 600$ ps and 29 for the remaining situations. When the cation is located into the cavity, the sulfonate groups partially replace the water molecules of the second hydration shell. The rdf of the free cation in solution and of the uncomplexed cation are identical whereas the rdf calculated for $t > 600$ ps tend to evolve toward that of the free cation in solution. The difference between the cation−water interaction energy of the free cation in solution and that of the inserted cation is equal to -861 ± 14 kJ mol^{-1}. This energy difference is due to the perturbed water structure in the second hydration shell of the inserted cation. This cation−water interaction energy is partially balanced by a more favorable calixarene−cation energy contribution when the cation is within the cavity. We calculate a difference in the calixarene−cation interaction energy of -540 ± 3 kJ mol^{-1} between the conformation with the cation inside the cavity and the conformation with the cation and the calixarene apart.

Figure 2c displays the integration of the calixarene−water oxygen radial distribution functions as a function of the distance. We observe that the cavity of the calixarene is solvated even in the presence of the ammonium cation. The integration of this distribution function up to 4 Å gives 2.8 and 3.2 water molecules inside the cavity for the inserted and uncomplexed cation, respectively. We note that the presence of the cation into the cavity does not affect dramatically the solvation of the calixarene. Figure 2d shows the number of cation atoms located at a distance *r* to the center of mass of the calixarene. We check that 100% of the atoms are found at 7.5 Å from the center of

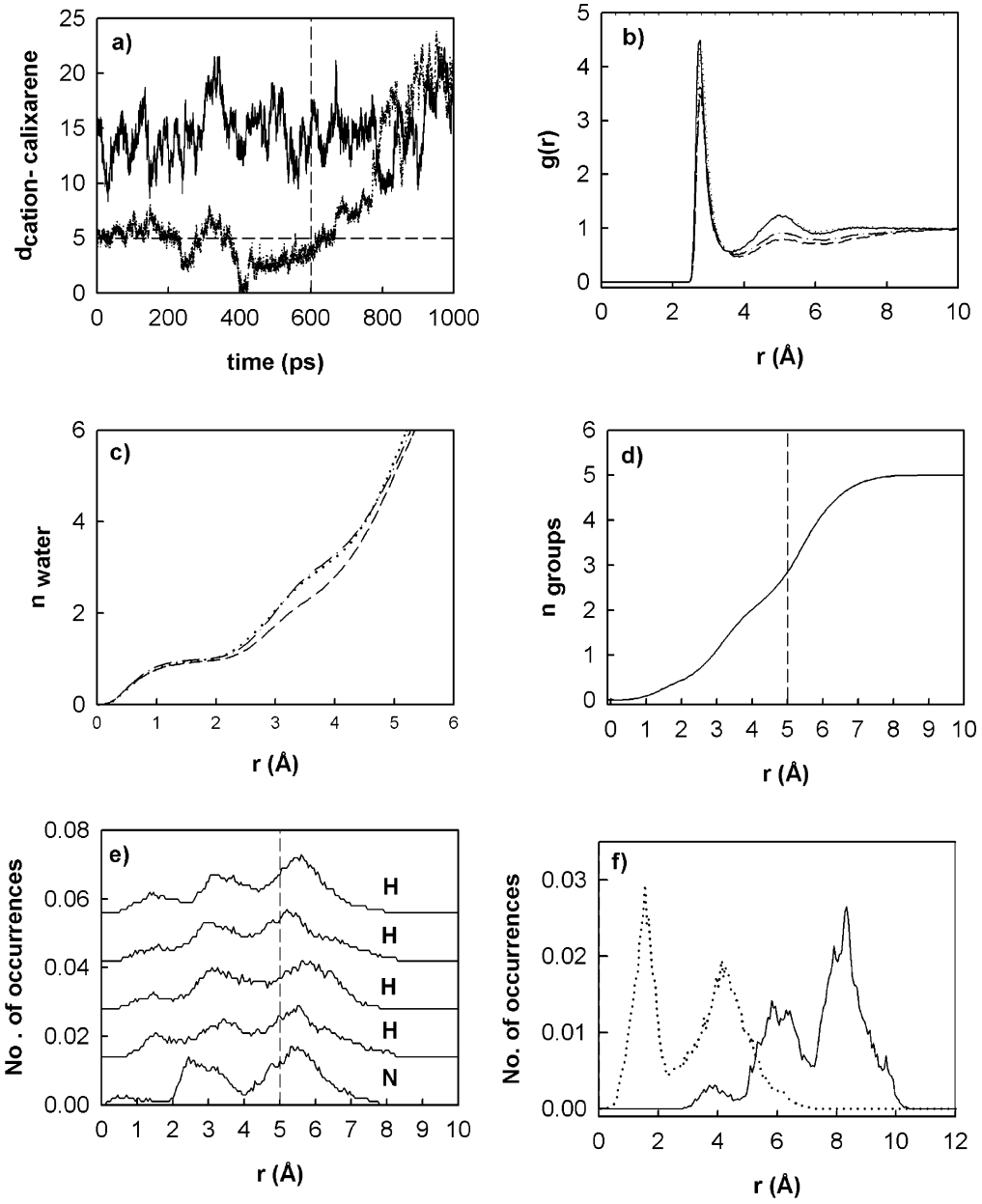

Figure 2. (a) Trajectories of the distance between the com of the calixarene and ammonium cation. The dotted line (lower curve) represents the trajectory of the ammonium cation initially placed into the cavity and the solid line (upper curve) concerns the MD calculation using a starting conformation with the host and guest apart. The dashed lines at $r = 5$ Å and at $t = 600$ ps represent the value of the radius of gyration of the calixarene and the time from which the NH_4^+ starts to leave the calixarene cavity, respectively. (b) Ammonium N−water oxygen rdfs: (—) free cation in solution; (− − −) MD for $t < 600$ ps; (−•−) MD for $t > 600$ ps; (•••) MD with the uncomplexed cation. (c) Integration of the calixarene−water oxygen rdf using the same symbols as in (b). (d) Integration of the distributions of the distance from each ammonium atom to the calixarene com. (e) Distributions of the distance from each atom of the NH_4^+ cation to the com of the calixarene. (f) Distributions of the distance between the com of the NH_4^+ and the com of the SO_3^- groups (dotted line) and between the NH_4^+ com and the com of the hydroxy groups (solid line).

mass of the macrocycle. At the limit size of the cavity (5 Å), we find 57% of the atoms. This means that the ammonium cation performs a good sampling of the cavity and of the region slightly above the sulfonate groups.

Part e of Figure 2 shows the distributions of the distance from each atom of the ammonium cation to the com of the calixarene up to 600 ps. These curves underline that the nitrogen atom covers a region of about 8 Å from the center of mass with two broad peaks. Figure 2f presents both the distributions of the distance from the com of the cation to the com of the sulfonate groups and to the com of the phenyl hydroxy groups. The distribution of the distance corresponding to the com of the lower rim varies from 3 to 10 Å with three distinct peaks whereas the distribution to the com of the upper rim extends over a range of 7 Å. It confirms that the ammonium cation has translational degrees of freedom inside the cavity. The fact that the distributions of the four hydrogen atoms shown in part e of Figure 2 are identical and extend over 8 Å indicate that the hydrogen atoms exchange their positions leading then to important degrees of freedom inside the cavity.

Even if these simulations from two different starting structures tend to show that the ammonium cation is not significantly complexed, these results are not definitive. We only see that the second hydration shell of the cation is perturbed upon insertion into the cavity. We also note a higher mobility of the inserted cation with translational and rotational degrees of freedom. One MD simulation underscores the leaving of the NH_4^+ cation from the cavity, with a final separation distance

of 20.7 Å. This large distance indicates that the cation does not form an inclusion complex nor an outer-sphere complex. We have indeed shown, in a previous work, that the distance from the com of the calixarene is only 5.9 ± 1.2 Å for the outer-sphere complex of La^{3+}.[12]

To provide a quantitative answer regarding the possible binding of the ammonium cation to the calixarene, we have developed a code to calculate the free energy of association or potential of mean force (PMF) as a function of the distance between the two centers of mass of the host and guest in the NpT ensemble. The PMF $w(r)$ function is calculated using the free energy perturbation (FEP) technique.[27,28] In the FEP methodology, the computation of the Gibbs free energy difference along the total reaction path in the NpT ensemble is divided in a number N_w of nonphysical contiguous states or windows connected by means of a coupling parameter λ, related to the calixarene−cation com distance, r_{ab}:

$$\Delta G_{FEP} = \sum_{i=1}^{N_w} w(r_{ab}(\lambda_i)) = \sum_{\lambda=0}^{1} -RT \ln \left\langle \frac{V \exp\left[-\frac{(H(r;r_{ab}(\lambda\pm\Delta\lambda)) - H(r;r_{ab}(\lambda)))}{RT} \right]}{\langle V \rangle} \right\rangle_{\lambda} \quad (2)$$

where R is the molar gas constant, T is the absolute temperature, and V is the volume of the system. $\langle\ \rangle$ denotes an isothermal−isobaric ensemble average reflecting state λ. $H(r,r_{ab}(\lambda))$ is the classical Hamiltonian corresponding to the state λ and depending only on the atomic coordinate set **r** and the fixed distance r_{ab} between the two centers of mass of the calixarene and ammonium cation. The constrained distance r_{ab} is now λ-dependent and varies according to the following relationship:

$$r_{ab}(\lambda) = \lambda r_{ab}(1) + (1 - \lambda) r_{ab}(0) \quad (3)$$

$H(r;r_{ab}(\lambda\pm\Delta\lambda)) - H(r;r_{ab}(\lambda))$ is averaged as the difference in energy between the perturbed configurations for which the host−guest distance is $r_{ab}(\lambda\pm\Delta\lambda)$ and the equilibrium configurations for which the host and guest are held at a fixed separation $r_{ab}(\lambda)$. This energy difference incorporates both the intrinsic interactions between the host and guest and the interactions between the two species and all the other molecules. In this energy calculation, we take into account the changes in the van der Waals interactions and in the contributions of the electrostatic energy calculated with the Ewald sum method. The constrained distance $r_{ab}(\lambda)$ is extended to $r_{ab}(\lambda+\Delta\lambda)$ and contracted to $r_{ab}(\lambda-\Delta\lambda)$ by moving each center of mass along the same vector. The distance from the com of the calixarene to the com of the ammonium cation is changed by ±0.125 Å from the starting structure to a distance of 9.0 Å and then by ±0.575 Å up to 13.175 Å.

In our FEP simulations, the perturbations are performed in both directions ("double-wide sampling") with 83 windows over the entire simulation. The difference between the forward ($+\Delta\lambda$) and backward ($-\Delta\lambda$) simulations gives a lower bound estimate of the error in the calculation. At each window, 10 ps of equilibration are followed by 30 ps of data collection with a time step of 1 fs. The total simulation time for a PMF calculation is about 3.4 ns.

Free energy profile calculated for the separation of the calixarene and ammonium molecules in dilute aqueous solution is shown in Figure 3a with the cumulative uncertainties. This profile is essentially repulsive up to 10.7 Å and then shows a plateau from the separation distance of 10.9 Å. In light of the PMF profile, the calixarene and ammonium molecules can be considered as not interacting. This means that the insertion of the NH_4^+ into the cavity is not energetically favorable and that the formation of an outer-sphere complex with an average distance between the host and the guest of about 10 Å is not very conceivable at the energetic level. The shallowness of the plateau of the free energy profile (−1.8 kJ mol^{-1}) confirms the fact that the solvent-separated calixarene−ammonium pair and the free molecules are not energetically distinct. Actually, the plateau of the PMF profile corresponds to a region where the ammonium cation is separated from the calixarene molecule by its two hydration shells. The ammonium N−water O radial distribution functions calculated both for the free cation in water and for the cation in a structure corresponding to that of the PMF plateau are identical.

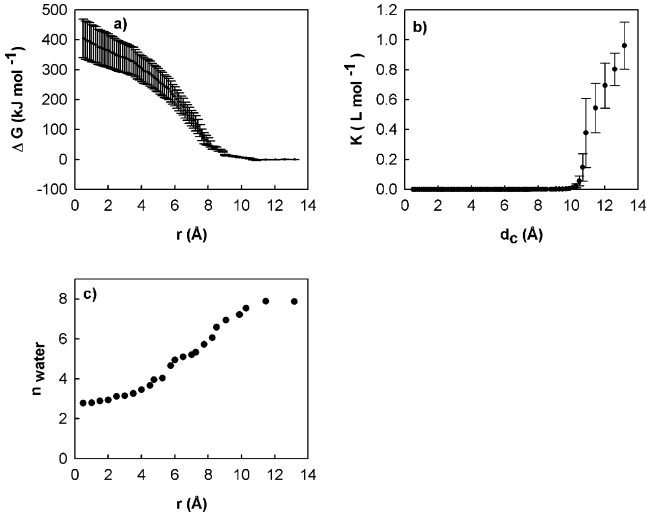

Figure 3. (a) Calixarene−NH_4^+ PMF profile as a function of the separation distance. The error bars correspond to the cumulative statistical uncertainties calculated in the backward and forward directions. (b) Association constant K calculated from eq 4 as a function of the association limit value d_c. (c) Number of water molecules present in the calixarene cavity as a function of the separation distance between the two centers of mass.

Part c of Figure 3 shows the number of solvent molecules inserted into the cavity of the calixarene as a function of the separation distance between the host and guest. When the separation distance is larger than 10.9 Å, we see that the hydration number of the calixarene cavity is the same as that calculated for the free calixarene in water.[12] For separation distances smaller than about 10 Å some bridging hydrogen bonds are formed between the water molecules of the first and second hydration shells of the ammonium cation and the calixarene anion. For larger separation distances, no water molecule is involved both in the hydration of the calixarene cavity and in the second hydration shell of the ammonium cation, indicating that the calixarene anion and the NH_4^+ cation are then well separated.

The PMF profile may be used to calculate[29] the association constant K using the following equation in the high-dilution limit

$$K = 4\pi N_a \int_0^{d_c} r^2 \exp\left(-\frac{w(r_{ab})}{kT} \right) dr \quad (4)$$

where $w(r_{ab})$ is the potential of mean force already defined in

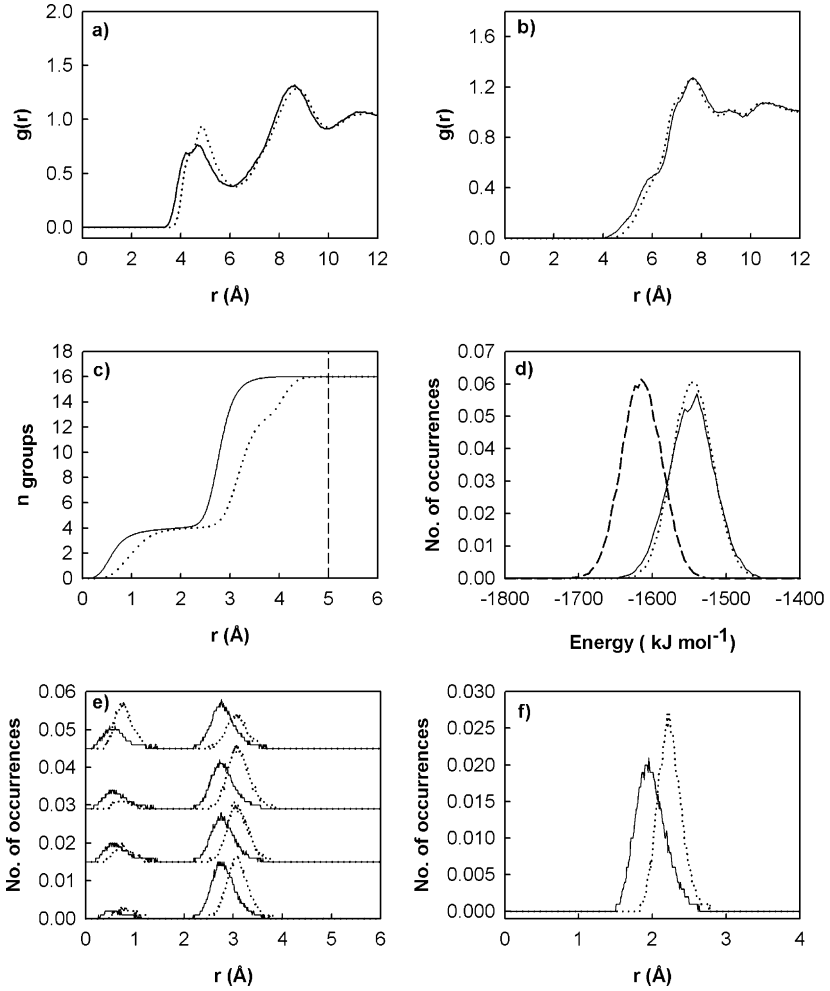

Figure 4. For all the figures, the solid line corresponds to the MD simulations using a UA model whereas the dotted line represents simulations carried out using as AA description. (a) Ammonium nitrogen−water oxygen rdfs. (b) Calixarene com−water oxygen rdfs. (c) Integration of the distributions of the distance from each interaction site of the Me_4N^+ to the com of the calixarene. (d) Distributions of the cation−calixarene energy contributions (kJ mol^{-1}). The dashed line corresponds to the interaction energy calculated at pH 7. (e) Distributions of the distance between each methyl group and the com of the calixarene. (f) Distributions of the distance between the nitrogen atom and the com of the calixarene.

(eq 3), k is Boltzmann's constant, and N_a is Avogadro's number. d_c is defined as the limit distance of association. The calculation of the association constant requires spherical shape for the two species. We have already shown, using the value of its asphericity coefficient, that the calixarene can be assimilated to a sphere. As expected, the ammonium cation is found to be spherical with an asphericity coefficient equal to 0.04. As the association constant is dependent on the cutoff value d_c, we report the results of the integration as a function of d_c in part b of Figure 3. Integration to the minimum value of the PMF plateau of the calixarene−ammonium system yields a K value of 0.38 L mol^{-1}. This small value and the large separation distance show that the cation is not complexed by the calixarene molecule. The calculation of the potential of mean force of the calixarene−ammonium system thus seems to confirm that there is no association between the calixarene and the ammonium cation in water, in agreement with the available microcalorimetric results.

3.2. Complexation of the Me_4N^+ Cation. This section presents the MD simulations of the binding of the calixarene with Me_4N^+ cation. The Me_4N^+ is modeled using both an all-atom model (AA) (Figure 1) and a united atom description (UA). In the AA approach, each atomic nucleus has an interaction site whereas in the UA approach, the methyl group of the Me_4N^+ is treated as one single interaction site. The parameters of the UA description are taken from ref 21.

Figure 4a, which displays the nitrogen−water oxygen rdf, shows that the first peak is slightly sharper with an AA description whereas the second shell is unchanged for the two approaches. However, the integration of the first peak gives identical results for the two models. We also observe that the hydration of the cavity is not sensitive to the model used. The calixarene com−water oxygen rdfs calculated using the two models are almost superimposed (Figure 4b). In addition, these rdfs indicate that the desolvation of the calixarene cavity is total. We show in Figure 4c the integrations of the distributions of the distance between the individual interaction sites of Me_4N^+ and the com of the calixarene for the AA and UA models. At $r = 5$ Å, we see that the two models yield a total insertion of the cation into the cavity, the insertion being slightly deeper with the UA model (Figure 1). Results shown in part d of Figure 4 and in Table 1 underline that the distributions of the cation−calixarene interaction energy are identical for the two models.

To check the rotational freedom of the cation inside the cavity, we have plotted in Figure 4e the distribution of the distance from the methyl groups to the com of the calixarene. These curves present two peaks whose location is identical for each methyl group. The two peaks show that each methyl group can

TABLE 1: Average Energy Components and Their Fluctuations (kJ mol^{-1}) for the Cation−Calixarene Interaction Energy

calixarene···cation energy	Me_4N^+			Et_4N^+		$MeNH_3^+$
	pH 2 (AA)	pH 2 (UA)	pH 7 (UA)	pH 2 (AA)	pH 7 (AA)	pH 2 (UA)
E_{vdw}	-45.6_{29}	-50.2_{29}	-49.7_{37}	-92.5_{38}	-84.5_{37}	-11.3_{25}
E_{ele}	-1495_{27}	-1501_{30}	-1615_{27}	-1511_{48}	-2184_{63}	-1452_{17}
E_{tot}	-1541_{30}	-1551_{33}	-1664_{31}	-1603_{52}	-2269_{67}	-1463_{20}

[a] E_{vdw} and E_{ele} correspond to the van der Waals and electrostatic interactions, respectively. E_{tot} is the sum of E_{vdw} and E_{ele}. The number -2269_{67} means -2269 ± 67.

take two positions relative to the calixarene com. The first peak, whose position is close to the calixarene com, shows that the methyl group is deeply inserted into the cavity. The second peak, with a larger amplitude, indicates that the methyl group is more often located toward the upper rim of the calixarene. This exchange between these two positions suggests a certain rotation of the Me_4N^+ cation into the cavity. This particularity is independent of the model. Parts e and f of Figure 4 confirm that the UA model predicts a slightly deeper insertion of the cation, the position of the peak for the distribution of the nitrogen atom differing by 0.3 Å according to the models. This rotation around the nitrogen atom is verified by the distribution of the distance of the nitrogen atom to the calixarene com which shows only one privileged position (Figure 4f). The two models do not show a difference regarding the structure of the complex, the solvation of the cavity, and the solvation of the cation. Moreover, calixarene−cation, cation−water, and calixarene−water interaction energies are, within the standard deviations, identical for the two models. This means that the calculation of the difference between the Gibbs free energies of complexation of Me_4N^+ and $MeNH_3^+$ may be carried out using a UA description for the methyl groups. For comparison, the calixarene−cation interaction energy components are reported in Table 1 as a function of the model, the pH, and the nature of the cation.

We also study the influence of the pH on the structure and on the energetics of the Me_4N^+ complex. At pH 2, all the phenolic hydroxy groups of the calixarene are protonated whereas at pH 7, one of the four hydroxy groups is deprotonated. Partial charges are then calculated over the whole calixarene anion with a total charge of -5. The simulations of the Me_4N^+ complex at pH 2 and 7 show no difference regarding the structure of the complex (insertion, solvation) and the mobility of the guest. The presence of a deprotonated hydroxy group on the lower rim of the calixarene changes the local organization of the intramolecular hydrogen bonds. In acidic solution, the network of the intramolecular hydrogen bonds is rigid whereas at pH 7 two different networks alternate with equal probability. The major differences we observe are the more negative contributions of the calixarene−cation and calixarene−water interactions at pH 7. The distributions of the calixarene−cation energy are given in part d of Figure 4 at pH 2 and 7 and the corresponding average energy values are reported in Table 1. We observe that the van der Waals Lennard Jones energy term in the calixarene−cation component is, within the standard deviations, the same at pH 2 and 7 whereas the electrostatic energy part becomes more negative at pH 7. The fact that the calixarene is more negatively charged at pH 7 leads to a more attractive calixarene−cation interaction energy that does not significantly change the structure of the complex.

3.3. Complexation of the Et_4N^+ Cation. The MD calculations of the complexes of the *p*-sulfonatocalix[4]arene with Et_4N^+ are performed at pH 2 and pH 7 using an AA description. The results are compared with those for the complexation with Me_4N^+ and Pr_4N^+.[12] We have already shown in a previous paper[12] that Et_4N^+ is the most inserted cation of the R_4N^+ series into the calixarene cavity (Figure 1). In the present work, we extend the study to show the insertion by calculating the number of alkyl groups within the cavity.

These simulations show that, whatever the pH, the tetraethylammonium cation is not completely inserted into the cavity of the calixarene. Figure 5a shows that at the limit of the cavity ($r = 5$ Å), the percentage of insertion is equal to 100% for Me_4N^+, 75% for Et_4N^+, and 38% for Pr_4N^+. The number of atoms inside the cavity is equal to 17, 21, and 15.5, respectively. The total calixarene−cation interaction energy calculated for Me_4N^+ and Et_4N^+ complexes in acidic solution is equal to -1541 ± 30 and -1603 ± 52 kJ mol^{-1}, respectively (Table 1). This decrease in energy is essentially due to the more negative van der Waals term for the Et_4N^+ complex. This result corroborates the differences observed as regards the inclusion of these cations into the calixarene cavity. The MD simulations show that the inclusion is more important in terms of the number of methylene and methyl groups for Et_4N^+ whereas it is less important for Pr_4N^+.

These MD results are consistent with the experimental enthalpies of complexation.[4,6] Part a of Figure 6 shows the $\Delta_r H°$ values and the number of atoms inserted into the host cavity. Interestingly, we observe a correlation between the enthalpy changes and the number of atoms inside the cavity. The MD simulations highlight the specific behavior of the Et_4N^+ complex within the R_4N^+ series, the most favorable $\Delta_r H°$ being associated with the largest number of atoms inserted into the cavity. Figure 6b suggests that from the calculation, for a given atom, of the number of atoms inserted into the cavity using molecular simulations, it may be possible to roughly estimate the $\Delta_r H°$ for the complexation of the other cations of the series.

As concerns the change in entropy, it is more difficult to explain it at the microscopic level. It is known that the desolvation of the macrocyclic host and of the cationic guest give positive contributions to $T\Delta_r S°$.[30,31] Our simulations show that 15 and 16 water molecules go back to the bulk upon complexation of Me_4N^+ and Et_4N^+, respectively. We also observe that the distributions of the distance from the methyl groups of the Et_4N^+ to the calixarene com present only one peak (Figure 5b) whereas the same distributions exhibit two distinct peaks for the Me_4N^+ (Figure 4e). This result reveals an important loss of degree of freedom for Et_4N^+ into the calixarene cavity at pH 2, which would lead to a negative contribution to $T\Delta_r S°$. However, the entropy contributions cannot be estimated from the present simulations.

The influence of the pH is shown on part b in Figure 5 from which we see that the distributions of the distance from the methyl groups of the Et_4N^+ cation to the com of the calixarene present two peaks at pH 7 and only one peak at pH 2. Furthermore, the location of the two peaks at pH 7 is the same for Me1 and Me4 and for Me2 and Me3 (see Figure 5b). This means that, at pH 7, the cation oscillates between two preferred positions leading to a restrained rotation of 90°. Its relative mobility is confirmed in Figure 5c, which shows a broadening

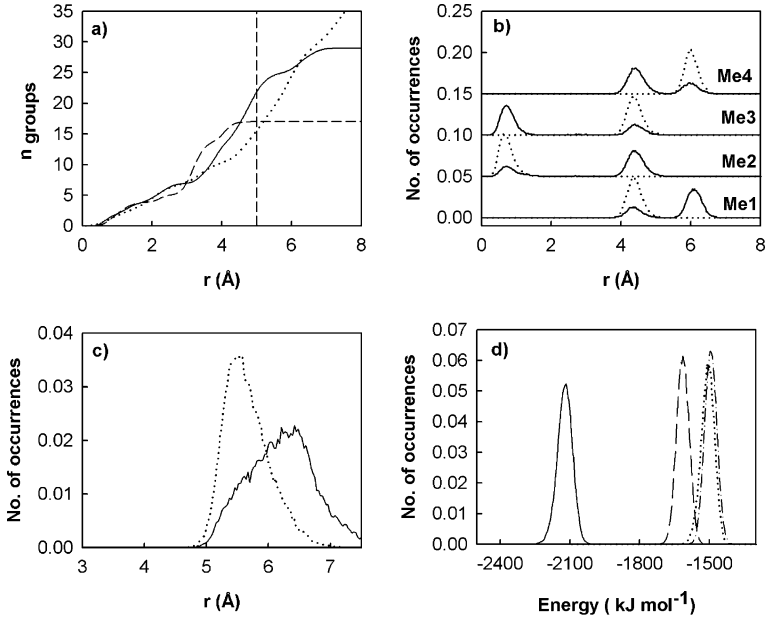

Figure 5. (a) Integration of the distributions of the distance from the interaction groups of the cation to the calixarene com: (− − −) Me_4N^+; (—) Et_4N^+; (•••) Pr_4N^+. (b) Distributions of the distance between each methyl group located at the end of an alkyl chain of the Et_4N^+ cation and the com of the calixarene. The dotted line is calculated at pH 2 and the solid line at pH 7. (c) Distributions of the distance from the com of the Et_4N^+ cation to the com of a SO_3^- group fo the calixarene at pH 2 (•••) and pH 7 (—). (d) Distributions of the cation−calixarene energy contribution (kJ mol^{-1}) calculated for the Et_4N^+ complex at pH 2 (•••) and at pH 7 (—) are added for comparison with the same distributions for the Me_4N^+ complex at pH 2 (−•−) and pH 7 (− − −).

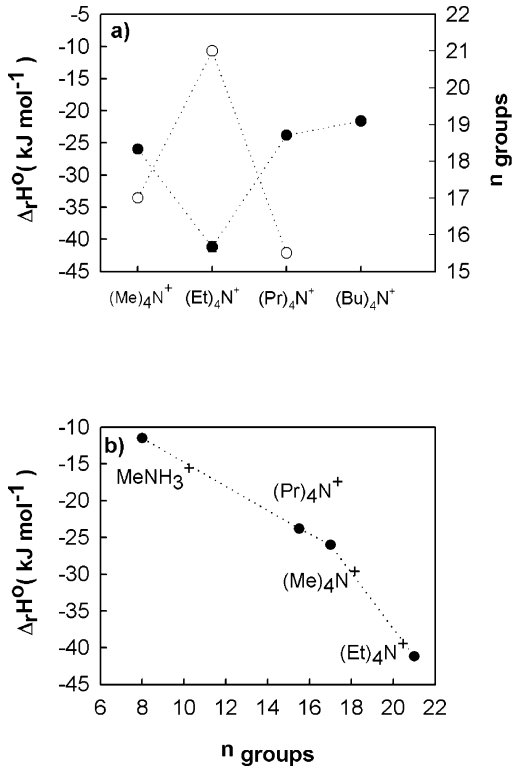

Figure 6. (a) $\Delta_r H°$ (●) and number of groups inserted into the host cavity (○) upon the complexation of R_4N^+ by the *p*-sulfonatocalix[4]-arene in water at pH 2. (b) Correlation between the $\Delta_r H°$ and n_{groups} values.

of the distribution of the distance between the com of the cation and of one sulfonate groups when changing pH from 2 to 7. This means that changing the calixarene charge can lead to some modification in the mobility of the Et_4N^+ cation without, however, significantly affecting the structure of the host and guest. The charge of the oxygen atoms of the SO_3^- groups becomes a little more negative at pH 7 (−1.01) compared to that (−0.89) at pH 2, leading to more important repulsions between these atoms at the upper rim. This may result in a slight opening of the upper rim, giving thus further degrees of freedom to the cation. However, this slight opening of the upper rim is too small to be observed from the components of the radius of gyration of the calixarene cavity.

We also observe a more negative calixarene−cation energy value at pH 7 than at pH 2. The difference in this energy contribution, mainly due to the electrostatic part, is equal to -666 ± 67 kJ mol^{-1}. As a comparison, we have also plotted the same distributions for the Me_4N^+ complex at pH 2 and pH 7. These curves show that the calixarene−cation energy contribution is more negative for the Et_4N^+ complex than for the Me_4N^+ complex, with a more pronounced difference at pH 7.

3.4. Binding with the $MeNH_3^+$ Cation. The MD simulations of the complexation of the calixarene with $MeNH_3^+$ are performed using a UA description for the methyl group (Figure 1). The trajectory of the distance between the com of the calixarene and cation, shown in Figure 7a, exhibits a value inferior to the radius of gyration of the cavity (5 Å) with some important fluctuations up to 5 Å between 430 and 510 ps whereas the same trajectory in the Me_4N^+ complex is constant around 1.98 ± 0.21 Å. Figure 7b shows that the location of $MeNH_3^+$ into the cavity is slightly deeper than that of Me_4N^+, with an average distance between the host and guest equal to 1.76 ± 0.35 Å. We deduce from this curve that the $MeNH_3^+$ is completely inserted into the cavity with a more important sampling of the calixarene cavity than that of Me_4N^+. From Figure 7c, it appears that the number of methyl groups and hydrogen atoms inserted into the cavity is always greater for Me_4N^+ than for $MeNH_3^+$. This is consistent with the fact that the enthalpy of complexation of Me_4N^+ is more negative than that of $MeNH_3^+$ [4,6] (Figure 6b).

Figure 7d presents the distributions of the distance from each interaction site of the $MeNH_3^+$ to the com of the calixarene.

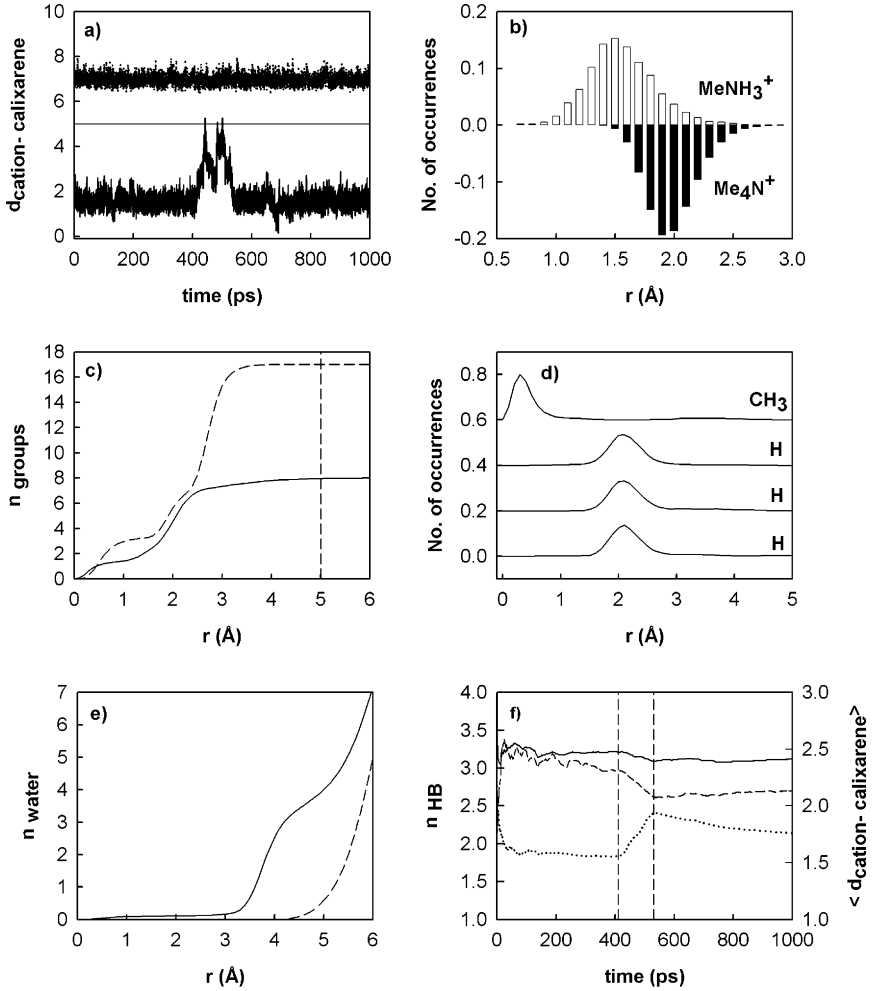

Figure 7. (a) Trajectories of the distance between the com of the $MeNH_3^+$ cation and the com of the calixarene (lower curve). The trajectory calculated in the Me_4N^+ complex is offset by 5 Å for clarity (upper curve). (b) Distributions of the distance between the centers of mass of the calixarene and cation. The distributions of the Me_4N^+ complex are multiplied by −1.0 for clarity. (c) Distributions of the number of interaction groups as a function of the dinstance to the com of the calixarene. The same distributions for the Me_4N^+ complex are shown for comparison (dashed line). (d) Distributions of the distance from each site of the $MeNH_3^+$ cation to the com of the calixarene. (e) Integration of the calixarene−water rdfs. The solid line represents the distributions calculated for the $MeNH_3^+$ complex, and the dashed line shows the distributions for the Me_4N^+ complex. (f) Trajectories fo the average number of hydrogen bonds between the $MeNH_3^+$ cation and the water molecules (—) and between the calixarene sulfonate groups and the water molecules giving hydrogen bonds with the cation (− − −). As a comparison, the average distance between the centers of mass of the calixarene and the cation (···) is shown.

The peak corresponding to the methyl group is located at 0.3 Å, suggesting that this group is within the calixarene cavity whereas the three hydrogen atoms of the ammonium are located toward the upper rim of the calixarene. Each interaction site presents only one peak, indicating that the $MeNH_3^+$ cannot rotate freely into the cavity, in contrast with the free rotation of the Me_4N^+. The complexed $MeNH_3^+$ has only translational degrees of freedom.

Part e of Figure 7 shows the integration of the calixarene−water oxygen rdfs. Interestingly, we see that the cavity of the calixarene is only partially desolvated upon complexation of $MeNH_3^+$. At $r = 4$ Å, an average number of 2.5 water molecules are present into the cavity whereas the desolvation is total upon complexation of Me_4N^+. This change in cavity solvation can be explained by the fact that the hydrogen atoms of the $MeNH_3^+$ can form hydrogen bonds with the oxygen atoms of the water molecules. To further analyze the formation of hydrogen bonds, we have plotted in part f of Figure 7 the time average number of hydrogen bonds formed between the $MeNH_3^+$ and the water molecules during the acquisition phase. We have also calculated the time average number of hydrogen bonds involving water molecules that simultaneously bond with the $MeNH_3^+$ and the SO_3^- groups of the calixarene molecule. This can be compared with the trajectory of the average distance between the com of the calixarene and cation. Whereas the distance between the cation and calixarene increases between 410 and 530 ps, the number of hydrogen bonds formed between the water molecules and the $MeNH_3^+$ alone or the $MeNH_3^+$ and the SO_3^- simultaneously decreases. The three curves show correlated behaviors between 410 and 530 ps. We check that new hydrogen bonds are temporarily created between the oxygen atoms of the SO_3^- groups and the hydrogen atoms of the $MeNH_3^+$, leading to a release of some water molecules and a slight desolvation of the sulfonate groups. As expected, this situation is unfavorable for the van der Waals part of the calixarene−cation energy contribution. The van der Waals LJ contribution does indeed become repulsive up to 43.9 kJ mol^{-1} between 410 and 530 ps, whereas it is, on average, negative and equal to −49.5 kJ mol^{-1}. During this period, the total cation−calixarene energy increases by 139 kJ mol^{-1}.

4. Conclusions

Throughout this paper, we report MD simulations of the complexation of the *p*-sulfonatocalix[4]arene with alkylammo-

nium cations in water. The potential of mean force of the calixarene−ammonium system has shown that the ammonium cation is not complexed by the calixarene molecule. This confirms the conclusions drawn from microcalorimetry.[4,6] In addition, two MD simulations differing in the initial location of the ammonium cation has allowed us to study the hydration of the host and guest for the two endpoints of the PMF profiles. As concerns the study of the Me_4N^+, Et_4N^+, Pr_4N^+, and $MeNH_3^+$ complexes, the MD simulations have highlighted a correlation between the experimental $\Delta_r H°$ values and the number of atoms inserted into the cavity of the calixarene. Furthermore, it has been shown that the specific behavior of Et_4N^+, which exhibits remarkably negative enthalpy and entropy of binding,[4] results from the inclusion of the largest number of atoms into the cavity accompanied by an important loss of degrees of freedom.

Concerning the influence of the acidity of the solution, we have not detected any major structural change of the complexes at acidic and neutral pH, except a different network of intramolecular hydrogen bonds for the lower rim. The deprotonation of one phenolic hydroxy group implies new charges that modify the calixarene−cation energy contribution, the values being more negative at pH 7 than at pH 2.

The MD simulations of the Me_4N^+ complex have shown that a description of the cation using a UA model gives similar results at the energetic and structural levels compared to the simulations using an AA description. The MD calculations of the $MeNH_3^+$ complex has shown that the methyl group is located inside the cavity whereas the hydrogen atoms of the ammonium point toward the water molecules. This work concerning the structures and the description of these two complexes constitutes a prerequisite for the forthcoming study in which we plan to calculate the difference between the Gibbs free energies for the association of the *p*-sulfonatocalix[4]arene with the Me_4N^+ cation and the $MeNH_3^+$ cation using a UA description.

References and Notes

(1) Sansone, F.; Segura, M.; Ungaro, R. In *Calixarenes 2001*; Asfari, Z., Böhmer, V., Harrowfield, J., Vicens, J., Eds.; Kluwer Academic Publishers: Dordrecht, 2001; Chapter 27 (see also references therein).

(2) Casnati, A.; Sciotto, D.; Arena, G. In *Calixarenes 2001*; Asfari, Z., Böhmer, V., Harrowfield, J., Vicens, J., Eds.; Kluwer Academic Publishers: Dordrecht, The Netherlands, 2001; Chapter 24 (see also references therein).

(3) Sussmann, J. L.; Harel, M.; Forlow, F.; Gefner, C.; Goldman, A.; Toker, L.; Silman, I. *Science* **1991**, *253*, 872.

(4) Bonal, C.; Morel, J. P.; Morel-Desrosiers, N. *J. Chem. Soc., Perkin. Trans.* **2001**, *2*, 1075.

(5) Bonal, C.; Morel, J. P.; Morel-Desrosiers, N. Unpublished results for the binding of the *p*-sulfonatocalix[4]arene with R_4N^+ in water at pH 7 and 298.15 K: thermodynamic properties for the binding with Me_4N^+ ($\Delta_r G° = -28.3$ kJ mol^{-1}; $\Delta_r H° = -24.6$ kJ mol^{-1}; $T\Delta_r S° = 3.7$ kJ mol^{-1}) and for the binding with Et_4N^+ ($\Delta_r G° = -31.2$ kJ mol^{-1}; $\Delta_r H° = -34.5$ kJ mol^{-1}; $T\Delta_r S° = -3.3$ kJ mol^{-1}).

(6) Perret, F.; Morel, J. P.; Morel-Desrosiers, N. *Supramol. Chem.* **2003**, *15*, 199.

(7) Lehn, J. M.; Meric, R.; Vigneron, J. P.; Cesario, M.; Guilhem, J.; Pascard, C.; Asfari, Z.; Vicens, J. *Supramol. Chem.* **1995**, *5*, 97.

(8) Stödeman, M.; Dhar, N. *J. Chem. Soc., Faraday Trans.* **1998**, *94*, 899.

(9) Conway, B. E. In *Thermodynamic and Transport Properties of Aqueous and Molten Electrolytes*; Conway, B. E., Bockris, J. O'M., Yeager, E., Eds.; Comprehensive Treatise of Electrochemistry, Vol. 5; Plenum Press: New York, 1983; Chapter 2.

(10) Tanford, C. *The Hydrophobic Effect*; Wiley: New York, 1980.

(11) Schneider, H. J.; Yatsimirsky, A. *Principles and Methods in Supramolecular Chemistry*, Wiley: Chichester, U.K., 2000; Chapter B.

(12) Mendes, A.; Bonal, C.; Morel-Desrosiers, N.; Morel, J. P.; Malfreyt, P. *J. Phys. Chem. B* **2002**, *106*, 4516.

(13) Wipff, G. In *Calixarenes 2001*; Asfari, Z., Böhmer, V., Harrowfield, J., Vicens, J., Eds.; Kluwer Academic Publishers: Dordrecht, The Netherlands, 2001; Chapter 17 (see also references therein).

(14) Cornell, W. D.; Cieplak, P.; Bayly, C. I.; Gould, I. R.; Merz, K. M., Jr.; Ferguson, D. M.; Spellmeyer, D. M.; Fox, T.; Caldwell, J. W.; Kollman, P. *J. Am. Chem. Soc.* **1995**, *117*, 5179.

(15) Ryckaert, J. P.; Ciccotti, G.; Berendsen, H. J. C. *J. Comput. Phys.* **1977**, *23*, 327.

(16) Tobias, D. J.; Klein, M. L. *J. Phys. Chem.* **1996**, *100*, 6637.

(17) Jorgensen, W. L.; Chandrasekhar, J.; Madura, J. D. *J. Chem. Phys.* **1983**, *79*, 926.

(18) Allen, M. P.; Tildesley, D. J. *The computer simulation of liquids*; Clarendon Press: Oxford, U.K., 1987.

(19) Breneman, C. P.; Wiberg, K. B. *J. Comput. Chem.* **1990**, *11*, 361.

(20) Schmidt, M. W.; Baldridge, K. K.; Boatz, J. A.; Elbert, S. T.; Gordon, M. S.; Jensen, J. J.; Koseki, S.; Matsunaga, N.; Nguyen, K. A.; Su, S.; Windus, T. L.; Dupuis, M.; Montgomery, J. A. *J. Comput. Chem.* **1993**, *14*, 1347.

(21) Jorgensen, W. L.; Gao, J. *J. Phys. Chem.* **1986**, *90*, 2174.

(22) Berendsen, H. J. C.; Postma, J. P. M.; van Gunsteren, A.; DiNola, A.; Haak, J. R. *J. Chem. Phys.* **1984**, *81*, 3684.

(23) Street, W. B.; Tildesley, D. J.; Saville, G. *Mol. Phys.* **1978**, *35*, 639.

(24) DL_POLY is a parallel molecular dynamics simulation package developed at the Daresbury Laboratory Project for Computer Simulation under the auspices of the EPSRC for the Collaborative Computational Project for Computer Simulation of Condensed Phases (CCP5) and the Advanced Reserach Computing Group (ARCG) at the Daresbury Laboratory.

(25) Chandra, A.; Chowdhuri, S. *J. Phys. Chem. B* **2002**, *106*, 6779.

(26) Chandra, A. *J. Phys. Chem. B* **2003**, *107*, 3899.

(27) Zwanzig, R. W. *J. Chem. Phys.* **1954**, *22*, 1420.

(28) Mezei, M.; Beveridge, D. L. *Ann. N. Y. Acad. Sci.* **1986**, *482*, 1.

(29) Prue, J. E. *J. Chem. Educ.* **1969**, *46*, 12.

(30) Smithrud, D. B.; Wyman T. B.; Diederich F. *J. Am. Chem. Soc.* **1991**, *113*, 5420.

(31) Marcus, Y. *Ion properties*; Marcel Dekker Inc.: New York, 1997.